063660

NASA TECHNICAL REPORT

NASA TR R-232

NASA TR R-232

AMPTIAC

DISTRIBUTION STATEMENT A
Approved for Public Release
Distribution Unlimited

A THEORETICAL AND EXPERIMENTAL INVESTIGATION OF THE OXIDATION OF MOLYBDENUM AT TEMPERATURES AT WHICH ITS TRIOXIDE IS VOLATILE

Reproduced From
Best Available Copy

by David R. Schryer and Gerald D. Walberg

Langley Research Center
Langley Station, Hampton, Va.

20020320 202

NATIONAL AERONAUTICS AND SPACE ADMINISTRATION • WASHINGTON, D. C. • MARCH 1966

NASA TR R-232

A THEORETICAL AND EXPERIMENTAL INVESTIGATION OF THE OXIDATION OF MOLYBDENUM AT TEMPERATURES AT WHICH ITS TRIOXIDE IS VOLATILE

By David R. Schryer and Gerald D. Walberg

Langley Research Center
Langley Station, Hampton, Va.

NATIONAL AERONAUTICS AND SPACE ADMINISTRATION

For sale by the Clearinghouse for Federal Scientific and Technical Information
Springfield, Virginia 22151 – Price $2.00

CONTENTS

A THEORETICAL AND EXPERIMENTAL INVESTIGATION OF THE OXIDATION OF MOLYBDENUM AT TEMPERATURES AT WHICH ITS TRIOXIDE IS VOLATILE

By David R. Schryer and Gerald D. Walberg
Langley Research Center

SUMMARY

A theoretical and experimental investigation of the oxidation of molybdenum to molybdenum trioxide at temperatures at which the trioxide is volatile has been carried out. A rate equation has been derived which includes the effects of mass-transfer parameters as well as chemical parameters and is applicable to any situation for which a mass-transfer coefficient can be obtained. The derived equation has been applied to previously reported rate data taken under laboratory conditions using air and oxygen-helium mixtures flowing at low subsonic velocities, and a set of values for the activation energy of the oxidation of molybdenum has been obtained. The average of these values is 8.51×10^7 J-(kg-mole)$^{-1}$ $\left(20.3 \text{ kcal-(g-mole)}^{-1}\right)$ with a standard deviation of 2.1 percent.

In addition, 32 molybdenum hemisphere-cylinder specimens have been oxidized in a Mach 2.1 heated airstream at a free-stream stagnation pressure of 1.07×10^6 N-m^{-2} (10.5 atm) and free-stream stagnation temperatures from 1765° K to 2120° K. The stagnation-point surface temperature and recession rate were determined for each of the specimens. The observed recession rates were compared with the corresponding values predicted theoretically by the derived rate equation and agreement within a factor of about 2 was obtained for most specimens. However, a few specimens ignited, exhibiting recession rates much greater than those predicted theoretically. The high recession rates associated with ignition were found to be the result of a sharp rise in surface temperature which caused some melting of the specimens in addition to their normal oxidation.

INTRODUCTION

Molybdenum differs from most other metals in that over an extended temperature range below the melting point of the metal its most stable oxide, molybdenum trioxide, is gaseous and, hence, nonprotective (ref. 1). The melting point of molybdenum is 2890° K, but the normal boiling point of its trioxide is 1428° K. Furthermore, under appropriate conditions the trioxide may be almost completely volatilized as much as several hundred

degrees below its normal boiling point. Whatever the conditions, there is a large temperature range over which a molybdenum surface situated in an oxygen containing environment is bare and, therefore, vulnerable to direct attack by oxygen.

The unprotected condition of molybdenum at high temperatures leads to very high oxidation rates (refs. 2, 3, and 4). These high oxidation rates impose a drain on the oxygen supply just adjacent to the molybdenum surface and, consequently, parameters affecting the replenishment of this supply – mass-transfer parameters – may be expected to influence the observed oxidation rate. It has been shown both theoretically (refs. 2 and 5 and Discussion of ref. 3) and experimentally (refs. 2, 3, 4, and 6) that this is in fact the case: the oxidation rate of molybdenum is, in general, dependent upon mass-transfer parameters as well as chemical parameters, although under certain environmental conditions one or the other set of parameters may predominate.

Because the oxidation rate of molybdenum at high temperatures is dependent upon both transport and chemical parameters, any equation which attempts to describe it must include the effects of both sets of parameters. Such an equation was derived theoretically in reference 2 for the special case of a specimen oxidizing in a flowing gas stream under conditions such that laminar boundary layers are established. The effects of mass transfer were introduced by means of certain simplifying assumptions which resulted in the appearance in the derived rate equation of an empirical proportionality "constant" which is actually a function of various environmental parameters. Thus, although the equation derived in reference 2 serves to illustrate the interaction of transport and chemical parameters and is suitable for the correlation of data taken under similar conditions, it is not suitable for the prediction of oxidation rates.

A theoretical rate equation similar to, but more general than, that presented in reference 2 is derived in the present report. In this treatment the experimental system is not specified and the effects of mass transfer are introduced by means of a mass-transfer coefficient rather than by recourse to the simplifying assumptions utilized in reference 2. The new rate equation retains the capabilities of that presented in reference 2 and, in addition, makes possible the prediction of oxidation rates for conditions for which the value of the mass-transfer coefficient can be obtained. The activation energy for the oxidation of molybdenum must, of course, also be known. The determination of both the activation energy and the mass-transfer coefficient is discussed in this report.

The present investigation has also included an experimental study for the purpose of obtaining molybdenum oxidation rate data under conditions more severe than the static and low subsonic conditions reported in the literature to date (refs. 2, 3, 4, and 6). This study has involved the oxidation of molybdenum hemisphere-cylinders in heated air-streams at a Mach number of 2.1 and a free-stream stagnation pressure of 1.07×10^6 N-m^{-2} (10.5 atm). The average steady-state stagnation-point surface

temperature of the test specimens varied from 1535° K to 2405° K. The experimentally determined oxidation rates were compared with those predicted theoretically by the rate equation derived in this report.

SYMBOLS

Wherever necessary the symbols and units used in the various references cited in this report have been changed to conform with those given in this section.

a speed of sound, meters-second^{-1}

a_o, a_1, a_2 parameters in equation (B6)

C concentration of oxygen, kilograms-meter^{-3}

$\bar{c}_p$ frozen specific heat at constant pressure, joules-kilogram^{-1}-^{o}K^{-1}

D diffusivity, meters^{2}-second^{-1}

D_o diffusivity coefficient (see eq. (B3))

d diameter, meters

E_a activation energy, joules-(kilogram-mole)$^{-1}$

H enthalpy, joules-kilogram^{-1}

h heat-transfer coefficient, kilograms-meter^{-2}-second^{-1}

h_D mass-transfer coefficient, kilograms-meter^{-2}-second^{-1}

K geometric index (see eq. (A1))

k oxidation rate at a point on a surface (expressed as oxygen consumed), kilograms-meter^{-2}-second^{-1}

k_{av} oxidation rate averaged over a surface (expressed as oxygen consumed), kilograms-meter^{-2}-second^{-1}

l	length of specimen, meters
$\dot{l}$	recession rate, meters-second^{-1}
m	molecular weight
$\dot{m}$	mass-transfer rate, kilograms-meter^{-2}-second^{-1}
N_{Le}	Lewis number, $\frac{N_{Pr}}{N_{Sc}}$
N_{Ma}	Mach number
N_{Nu}	Nusselt number, $\frac{h\bar{c}_p x}{\kappa}$
N_{Pr}	Prandtl number, $\frac{\mu\bar{c}_p}{\kappa}$
N_{Re}	Reynolds number, $\frac{\rho u_e x}{\mu}$
$N_{Re,w}$	modified Reynolds number, $\frac{\rho_w u_e x}{\mu_w}$
N_{Sc}	Schmidt number, $\frac{\mu}{\rho D}$
n	temperature exponent (see eq. (B3))
P_1	mass-transfer parameter, assumed in reference 2 to be constant
p	pressure, newtons-meter^{-2}
p_o	standard pressure, newtons-meter^{-2} (see eq. (B3))
q	aerodynamic heat flux, joules-meter^{-2}-second^{-1}
R	universal gas constant, joules-(kilogram-mole)$^{-1}$-^{o}K^{-1}
r	radius of cross section of body of revolution, meters
T	temperature, ^{o}K
T_o	standard temperature, ^{o}K (see eq. (B3))

$\overline{T}$	average surface temperature, ^{o}K
$\overline{T}_{30-40}$	average of stagnation-point surface temperature at 30 and 40 seconds, ^{o}K
$\overline{U}$	average speed of oxygen molecules, meters-second^{-1}
u	component of velocity parallel to surface, meters-second^{-1}
V	molar volume of a gas at its normal boiling point, meters^{3}-(kilogram-mole)$^{-1}$
v	component of velocity normal to surface, meters-second^{-1}
w	mass fraction
X	mole fraction
x	coordinate parallel to surface, meters
y	coordinate normal to surface, meters
δ_C	concentration boundary-layer thickness, meters
θ	normalized enthalpy, defined by equation (A5)
κ	thermal conductivity, joules-meter^{-1}-second^{-1}-$^{o}K^{-1}$
μ	viscosity, kilograms-meter^{-1}-second^{-1}
ρ	density, kilograms-meter^{-3}
ϕ	normalized mass fraction, defined by equation (A6)

Subscripts:

e	condition at edge of boundary layer or other mass-transfer path
He	helium
i	numerical index

Mo	molybdenum
O_2	oxygen
t	stagnation condition
w	condition adjacent to wall

THEORETICAL ANALYSIS

Derivation of Rate Equation

It has been shown by Gulbransen, Andrew, and Brassart (ref. 3) that, at temperatures at which the reaction products are volatile, the rate determining mechanism for the oxidation of molybdenum involves mobile adsorption of oxygen on the molybdenum surface. The rate equation for this mechanism according to Laidler, Glasstone, and Eyring (ref. 7) is

$$k = C_w\left(\frac{RT_w}{2\pi m_{O_2}}\right)^{1/2} \exp\left(\frac{-E_a}{RT_w}\right) \tag{1}$$

By making use of the expression given by the kinetic theory of gases for the average molecular speed $\overline{U}$ (ref. 8), this equation can be rewritten as

$$k = \frac{C_w\overline{U}}{4} \exp\left(\frac{-E_a}{RT_w}\right) \tag{2}$$

In this form the rate equation for mobile adsorption can be seen to be identical to that derivable from simple collision theory. (See Discussion of ref. 3.)

An alternate expression for equation (2) in terms of the mass fraction, rather than the concentration, of oxygen at the surface is

$$k = \frac{{}^{w}O_{2,w}\rho_w\overline{U}}{4} \exp\left(\frac{-E_a}{RT_w}\right) \tag{3}$$

For steady-state conditions the rate of consumption of oxygen at the surface must equal the rate of transport of oxygen to the surface – that is,

$$k = \dot{m}_{O_2,w} \tag{4}$$

The oxygen transport rate may be expressed in terms of a mass-transfer coefficient as

$$\dot{m}_{O_2,w} = h_D\left(w_{O_2,e} - w_{O_2,w}\right) \tag{5}$$

Therefore,

$$k = h_D\left(w_{O_2,e} - w_{O_2,w}\right) \tag{6}$$

The parameter $w_{O_2,w}$ which appears in equations (3) and (6) will, in general, be unknown. Therefore, it is eliminated by combining the two equations; the resulting equation is

$$k = \frac{w_{O_2,e} h_D \frac{\overline{U}}{4} \exp\left(\frac{-E_a}{RT_w}\right)}{\frac{\overline{U}}{4} \exp\left(\frac{-E_a}{RT_w}\right) + \frac{h_D}{\rho_w}} \tag{7}$$

Equation (7) is a general expression for the rate of oxidation of molybdenum at temperatures at which its trioxide is volatilized; it includes the effects of both chemical and transport parameters. Under the appropriate conditions either of these two sets of parameters may predominate; for such conditions one or the other of two limiting modifications of equation (7) will result. If the transport term h_D/ρ_w is much larger than the chemical term $\frac{\overline{U}}{4} \exp\left(\frac{-E_a}{RT_w}\right)$, equation (7) reduces to

$$k = w_{O_2,e} \rho_w \frac{\overline{U}}{4} \exp\left(\frac{-E_a}{RT_w}\right) \tag{8}$$

which is the limiting equation for chemical control.

On the other hand, if the transport term is much smaller than the chemical term, equation (7) becomes

$$k = w_{O_2,e} h_D \tag{9}$$

which is the limiting equation for transport control.

In the application of equations (7) and (9) to specific problems it is extremely difficult to obtain creditable values for the parameters ρ_w and h_D if the pressure and mean molecular weight of the gas adjacent to the molybdenum surface are significantly different from their values in the free stream or reservoir. (The designation of the undepleted main body of the gas as the "free stream" or the "reservoir" depends upon whether the gas is flowing or essentially static.) The conversion of oxygen to molybdenum

trioxide by reaction with the molybdenum surface inevitably results in changes in the pressure and mean molecular weight of the gas mixture adjacent to the surface. These changes are negligibly small if the reaction rate is chemically controlled. For more rapid reaction rates the extent of the changes can be reduced by the incorporation of inert diluents in the oxidizing gas mixture. If a sufficiently large fraction of inert constituents is used, the pressure and mean molecular weight of the gas mixture can be maintained effectively uniform even when the reaction proceeds rapidly enough to be predominantly transport controlled. Because of these considerations it will be assumed throughout this report that the pressure and mean molecular weight of the oxidizing gas mixture are uniform in all cases.

In view of the foregoing assumption, equation (7) can be rewritten for the special case of systems where the temperature of the gas mixture is uniform. For such systems

$$\rho_e = \rho_w = \rho \tag{10}$$

and equation (7) becomes

$$k = \frac{C_e \frac{h_D}{\rho} \frac{\overline{U}}{4} \exp\left(\frac{-E_a}{RT_w}\right)}{\frac{\overline{U}}{4} \exp\left(\frac{-E_a}{RT_w}\right) + \frac{h_D}{\rho}} \tag{11}$$

For systems for which the temperature is not uniform the more general equation (7) must be used.

Equation (11) is very similar to a rate equation derived in reference 2 for the special case of oxidation in a flowing gas stream of uniform density under conditions such that laminar boundary layers are established. The two equations differ only in the transport term which is h_D/ρ in equation (11) and is $P_1 D/\delta_C$ in the equation derived in reference 2. It can be seen that the parameter P_1 which is assumed in reference 2 to be a constant is actually a variable defined by the equation

$$P_1 = \frac{h_D \delta_C}{\rho D} \tag{12}$$

All the parameters in equations (7) and (11), with the exception of the activation energy, can be calculated for many situations of interest. (See appendixes A and B.) Therefore, once the activation energy has been determined, these equations can be used for the prediction of oxidation rates for such situations. The determination of the activation energy from previously reported data is discussed in the next section.

Determination of Activation Energy From Average Oxidation-Rate Data for Flat-Plate Specimens

Data on the oxidation rate of molybdenum taken under controlled laboratory conditions are reported in reference 2. The specimens tested were thin flat plates of molybdenum which were oxidized in a tube furnace in slowly flowing gas streams with flow velocities of 1.76 to 8.00 m-sec^{-1}. The specimens were all alined parallel to the flow. The exhaust pressure of the system was atmospheric for all tests. The surface temperature of the specimens ranged from 1069° K to 1644° K. Three different gas mixtures were used: Air; 21.5 percent O_2, 78.5 percent He; and 13.6 percent O_2, 86.4 percent He.

The reaction conditions and gas mixtures employed in the study reported in reference 2 were such that the density could be considered uniform throughout the boundary layer and, thus, the appropriate rate equation is equation (11). However, since the oxidation rates reported in reference 2 are averages over the entire surface of the specimens, rather than values for particular points on the surface, equation (11) must be modified somewhat in order to be applicable to these data. This modification is accomplished in the following paragraphs.

Since the oxidation rate is very nearly constant over any narrow strip across the surface of a specimen which is located a distance x from the leading edge, the mean value theorem of the integral calculus gives the average oxidation rate as

$$k_{av} = \frac{1}{l} \int_0^l k \, dx \tag{13}$$

To utilize equation (13) it is necessary to have an expression for k as a function of x which, in turn, requires an expression relating h_D and x. In appendix A, h_D for the present case is shown to be given by the equation

$$h_D = 0.332 \, \rho \, \frac{D_w}{x} \sqrt[3]{N_{Sc}} \sqrt{N_{Re}} \tag{14}$$

From the definition of the Reynolds number and equations (11), (13), and (14),

$$k_{av} = \frac{1}{l} \int_0^l \frac{0.332 C_e D_w \frac{\overline{U}}{4} \sqrt[3]{N_{Sc}} \left(\frac{\rho u_e}{\mu x}\right)^{1/2} \exp\left(\frac{-E_a}{RT_w}\right)}{\frac{\overline{U}}{4} \exp\left(\frac{-E_a}{RT_w}\right) + 0.332 D_w \sqrt[3]{N_{Sc}} \left(\frac{\rho u_e}{\mu x}\right)^{1/2}} dx \tag{15}$$

Integration of equation (15) produces the desired expression for the average oxidation rate:

$$k_{av} = \frac{2(0.332)D_w C_e \sqrt[3]{N_{Sc}}}{\left(\frac{\mu l}{\rho u_e}\right)^{1/2}} \left\{ 1 - \frac{0.332 D_w \sqrt[3]{N_{Sc}}}{\left(\frac{\mu l}{\rho u_e}\right)^{1/2} \frac{\overline{U}}{4} \exp\left(\frac{-E_a}{RT_w}\right)} \log_e \left[1 + \frac{\left(\frac{\mu l}{\rho u_e}\right)^{1/2} \frac{\overline{U}}{4} \exp\left(\frac{-E_a}{RT_w}\right)}{0.332 D_w \sqrt[3]{N_{Sc}}} \right] \right\} \quad (16)$$

Application of equation (16) to the data presented in reference 2 yields a set of values for the activation energy, one value for each test. (See table II.) Only the data for temperatures of 1300° K and above have been considered, since these are the data for which the molybdenum trioxide reaction product was completely volatilized.

EXPERIMENTAL STUDY

Facility and Test Conditions

All tests performed in this study were carried out in the Langley 11-inch ceramic-heated tunnel (ref. 9). For all tests the oxidizing gas was air, the stagnation pressure of the airstream was 1.07×10^6 N-m^{-2} (10.5 atm), and the Mach number was 2.1. The free-stream stagnation temperature varied among the tests from 1765° K to 2120° K; the values for the individual tests are presented in table I.

Test Specimens

All specimens tested were solid 0.0095-m-diameter hemisphere-cylinders which were machined from sintered molybdenum of a purity of 99.98 percent. The specimens were mounted in a water-cooled sting which could be inserted into and retracted from the heated airstream while the tunnel was in operation.

Photographs of a typical specimen before testing are presented in figure 1. Figure 1(a) shows the specimen unmounted and figure 1(b) shows the specimen mounted in the detachable copper nose of the water-cooled sting.

Temperature Measurement

The surface temperature of the specimens tested in this investigation was measured with a photographic pyrometer. The theory and technique of photographic pyrometry are discussed in references 10 and 11. The pyrometer used in the present study was the prototype model described in reference 10. In this reference the precision of this instrument is estimated to be about ±2 percent. In practice it has been found that precision of

this order is attainable only under idealized conditions. A more realistic estimate of the precision of the surface temperatures presented in this report (table I) is ±4 to ±5 percent.

Experimental and Analytical Techniques

The operational procedure for most of the tests made in this investigation consisted of starting the tunnel, allowing time for stable operation to be achieved, and then rapidly inserting a test specimen into the heated airstream where it was rigidly held for a predetermined length of time at the end of which it was rapidly retracted. The only exceptions to this procedure involved the retraction before the completion of their scheduled test time of a few specimens which unexpectedly ignited.

For each specimen tested the surface temperature and recession rate were determined. Because both of these parameters varied across the surface of the specimens, they were determined at a single common point – the stagnation point.

The stagnation-point surface temperature of each specimen was measured at 30 sec after insertion of the specimen into the heated airstream and every 10 sec thereafter until the end of the test. Preliminary tests in which temperatures were read at frequent intervals up to 30 sec showed that the stagnation-point surface temperature rose rapidly from the ambient value for the first few seconds and then, except for the few specimens that ignited, gradually tapered off to a steady-state value which was generally reached between 20 and 30 sec. The temperature then remained relatively constant (within ±5 percent for most specimens) until the end of the test.

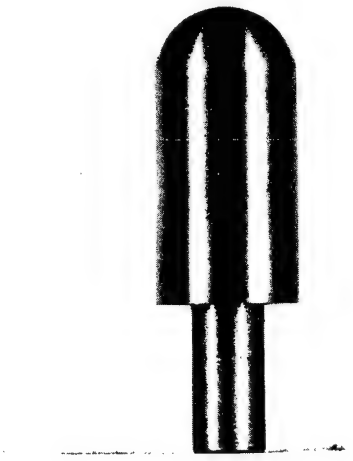

(a) Unmounted. L-64-11,722

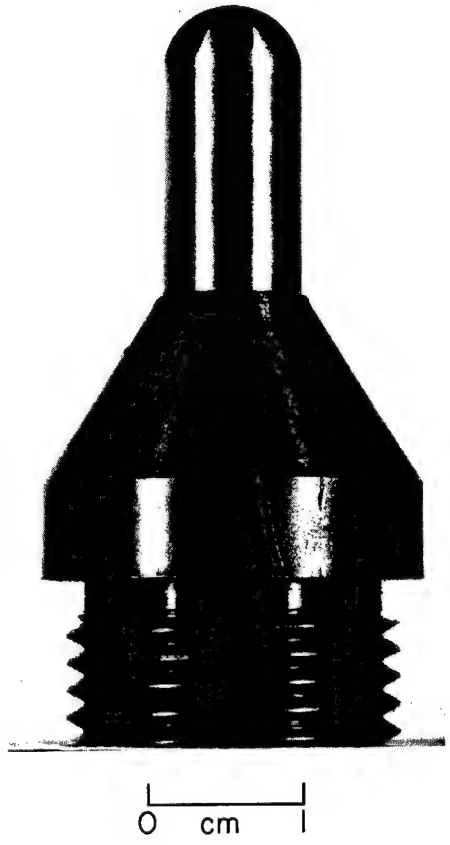

(b) Mounted. L-64-11,723

Figure 1.- Typical hemisphere-cylinder test specimen.

The recession rates of the specimens were not measured directly but were determined from their total recessions by a technique which is described in the following paragraphs. The total recession of each specimen was determined by measuring its total length with a micrometer before and after testing.

At the steady-state temperatures involved in this investigation the rate of oxidation of molybdenum, at a given temperature, is linear with respect to time. However, because there was a significant transient period before the specimens reached their steady-state temperatures, meaningful recession rates could not be calculated simply by dividing the total recession of each specimen by its test time; some compensation for the recession which occurred during the transient period was necessary. This compensation was achieved by running a set of seven 40-sec tests at various free-stream stagnation temperatures. (See table I(a).) (Although all the specimens previously tested reached their steady-state temperatures within 30 sec, an additional 10-sec margin was allowed.) The average of the stagnation-point surface temperatures at 30 and 40 sec, designated $\overline{T}_{30-40}$, was determined for each specimen. In figure 2 the total stagnation-point recession of each of the seven specimens is plotted against the corresponding value of $\overline{T}_{30-40}$. Although some scatter is evident among the data, a linear trend is apparent and, consequently, a straight line was fitted to the data by the least squares method. The ordinate of each point on this line was then assumed to represent the recession in the first 40 sec of any test specimen with a value of $\overline{T}_{30-40}$ equal to the abscissa of the point.

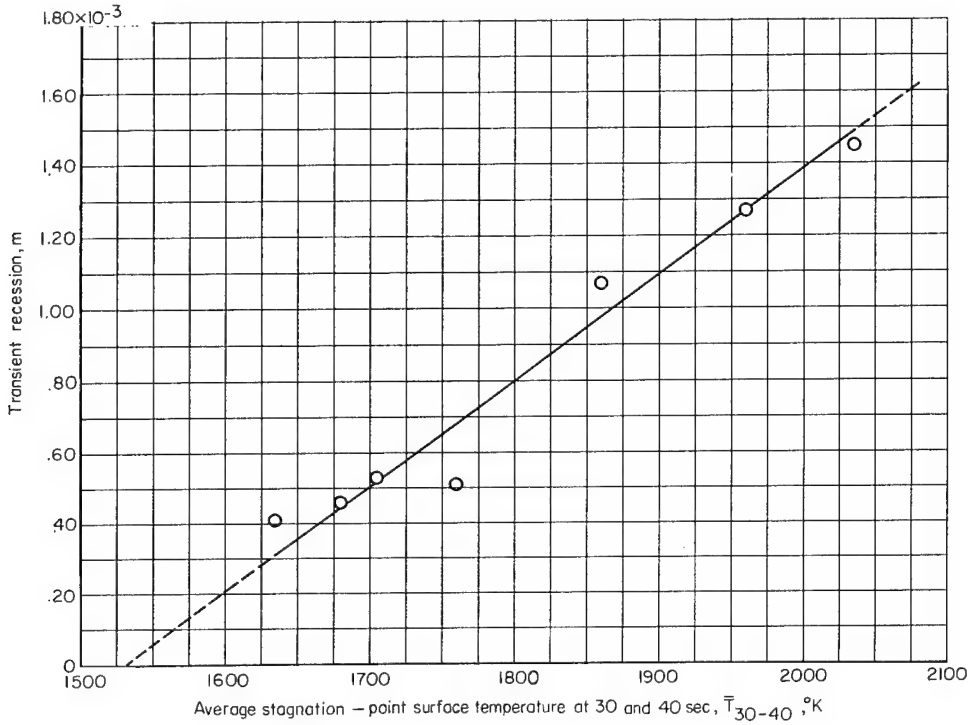

Figure 2.- Variation of transient recession with average stagnation-point surface temperature.

Twenty-two specimens were tested for periods longer than 40 sec; twenty-one of these oxidized normally and did not ignite. For each of these specimens $\overline{T}_{30-40}$ and, also, the average stagnation-point surface temperature from 40 sec to the end of the test $\overline{T}$ were determined. (For brevity, the latter temperature hereinafter will be referred to simply as the "average surface temperature.") From figure 2 the transient recession of each test specimen corresponding to its $\overline{T}_{30-40}$ value was obtained. This transient recession was then subtracted from the specimen's total recession and the difference was divided by the total test time minus 40 sec. The resultant value was assumed to be the steady-state recession rate of the specimen corresponding to the average surface temperature $\overline{T}$.

The technique just described is admittedly less precise than are the various techniques conventionally employed in the laboratory for the determination of reaction rates, techniques such as continuous weighing, resistance change measurement, and oxygen loss monitoring. However, none of these conventional techniques were applicable to the environment used.

It can be seen from figure 2 that the actual recession of a specimen in 40 sec may deviate as much as 0.00017 m from the value given by the least squares line. From table I(b) and figure 2 it can be determined that the difference between the transient recession given by the least squares line and the total recession, for the specimens tested longer than 40 sec, varies from 0.00035 m to 0.00310 m. Thus, the uncertainty in the recession rates determined varies among the specimens, ranging from at least 5 percent to 49 percent or greater.

The technique used to determine the recession rates of the specimens which oxidized normally required significant modification for the determination of recession rates due to ignition. The rapid deterioration which resulted from ignition was in every instance accompanied by a rapid rise in surface temperature to a value more than 500° K above the average preignition temperature. Thus, the entire preignition period, which varied in duration from 23 to 130 sec, constituted a transient period for which compensation was necessary.

This compensation was achieved as follows. The duration and average temperature of the preignition period were determined from the pyrometric film records for each specimen which ignited.[1] (The temperature was averaged by numerical integration using

[1]In one test in which ignition occurred the specimen (specimen 29) was not immediately retracted but was allowed to remain in the heated airstream for observation. The specimen receded rapidly for about 21 sec after the onset of ignition and then reverted back to normal oxidation until the end of the test. The duration and average temperature of this postignition period of normal oxidation were included with the specimen's corresponding preignition values.

the trapezoid rule; temperatures below 1428° K were not considered.) The theoretical recession rate associated with each specimen's average preignition temperature was obtained from equation (7).[2] This rate was then multiplied by the specimen's preignition time to yield the theoretical preignition recession. Each specimen's ignition recession rate was then determined by subtracting its theoretical preignition recession from its measured total recession and dividing the difference by the duration of ignition. The ignition recession rates determined by this technique are probably low for the following reasons: (1) The nose of each specimen which ignited assumed an irregular configuration. In no case was the center of the nose the farthest protruding point when the specimen lengths were measured after testing. Thus, at least one point of each specimen, the center of its nose, underwent a greater recession than the specimen's measured total recession. (2) As pointed out in the section "Results and Discussion," equation (7), the rate equation from which each specimen's preignition recession was theoretically determined, yields values higher than those which have been observed experimentally in the preignition temperature range. (3) The pyrometric film records from which the ignition times were determined yield readings about 1 sec apart and, therefore, the duration of ignition is uncertain in each case by about 2 sec. The ignition durations reported in table I(c) are the maximum values derivable from the film records.

RESULTS AND DISCUSSION

Determination of Activation Energy

Table II reproduces from reference 2 certain data regarding the oxidation of thin flat plates of molybdenum to molybdenum trioxide at temperatures and flow rates at which the trioxide is completely volatilized.[3] Also presented in this table are values of the activation energy for this reaction calculated from these data by means of equation (16); one value of the activation energy is presented for each data point. The data presented

[2]Equation (7) as presented yields the oxidation rate in kilograms of oxygen consumed per meter^2 of molybdenum surface per second. This oxidation rate was converted to the recession rate of the surface in meters per second by the following equation:

$$\dot{l} = \frac{2m_{Mo}}{3m_{O_2}\rho_{Mo}} k$$

[3]For consistency with the conventions of the present report the values of these data have been converted to the mksK system of units and the oxidation rates have been expressed in terms of the mass rate of oxygen consumed rather than the mass rate of molybdenum lost.

in table II are divided among five experimental series comprising five different mass flow rates and three gas mixtures: air and two oxygen-helium mixtures. As demonstrated in reference 2 all oxidation rates presented were to some extent transport controlled.

Table III presents the average value of the activation energy for each test series as calculated by equation (16) and also as calculated by a corresponding integrated rate equation derived in reference 2. In addition, table III presents the overall average value of the activation energy and the percent standard deviation from this average for each of the two rate equations considered. The percent standard deviation obtained by using equation (16), 2.1 percent, is an improvement over the value of 5.7 percent obtained with the integrated rate equation presented in reference 2. (The value of 3.6 percent given in reference 2 is the mean deviation and not the standard deviation.)

It can be seen from table III that not only does the use of equation (16) yield more consistent values for the activation energy when all the experimental data are considered together but it also significantly reduces the differences among the average values for the individual series. The maximum difference in the average value of the activation energy between two series obtained by using equation (16) is 0.16×10^7 J-(kg-mole)$^{-1}$, whereas with the equation in reference 2 it is 0.86×10^7 J-(kg-mole)$^{-1}$.

The overall mean value of the activation energy as calculated by equation (16) is 8.51×10^7 J-(kg-mole)$^{-1}$ (or 20.3 kcal-(g-mole)$^{-1}$) and as calculated by the equation from reference 2 it is 8.95×10^7 J-(kg-mole)$^{-1}$ (or 21.3 kcal-(g-mole)$^{-1}$). The former agrees within 3 percent and the latter agrees within 8 percent with the value 8.25×10^7 J-(kg-mole)$^{-1}$ (19.7 kcal-(g-mole)$^{-1}$) obtained by Gulbransen, Andrew, and Brassart (ref. 3) from an Arrhenius plot of experimental data taken by them. In general, the use of this type of plot for the determination of the activation energy of a material which forms a volatile oxide is unreliable due to the possible effects of transport parameters on the measured oxidation rates (refs. 2 and 5). However, when the data plotted have been obtained under predominantly chemically controlled conditions, this source of error is eliminated. Gulbransen, Andrew, and Brassart were able to obtain some data under chemically controlled conditions and only these data were considered in their determination of the activation energy.

It is apparent from the results just presented that equation (16) reduces the data of reference 2 more successfully than does the integrated rate equation presented in that reference.

Recession-Rate Data for Hemisphere-Cylinder Specimens

The recession rates and corresponding average surface temperatures of the molybdenum hemisphere-cylinder specimens tested in the present investigation – both those

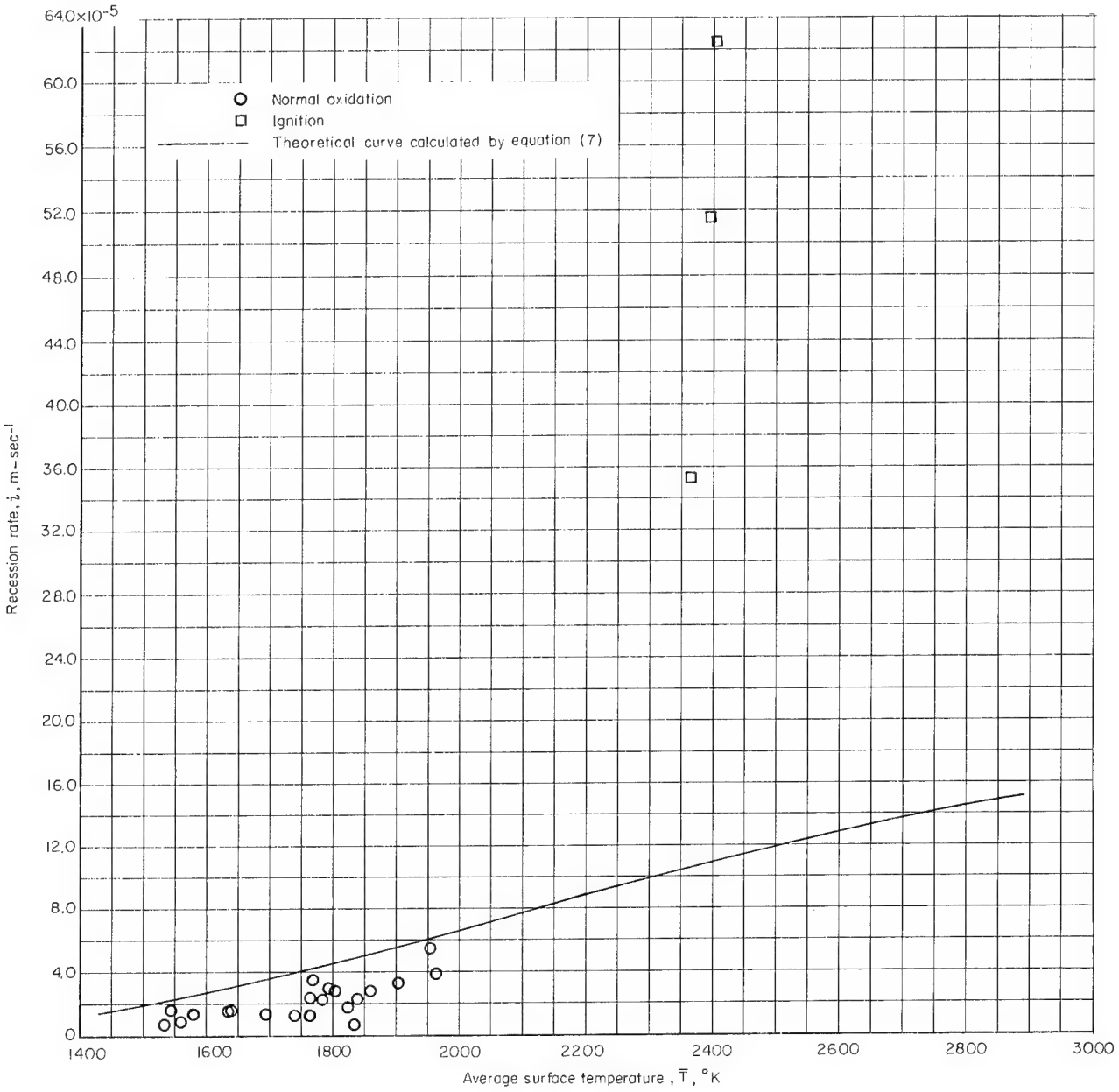

Figure 3.- Variation of recession rate with surface temperature.

that behaved normally and those that ignited – are listed in table I and plotted in figure 3. Also plotted in figure 3 is a theoretical curve of recession rate as a function of surface temperature calculated by means of equation (7) and based on the specimen configuration and test conditions utilized. This curve extends from 1428° K, the normal boiling point of molybdenum trioxide, to 2890° K, the melting point of pure molybdenum.

It can be seen that the nonignition data broadly follow the theoretical curve over the temperature range covered by the data although the data points all lie somewhat below the curve. The degree of scatter exhibited by the data is consistent with the estimated uncertainty of the measured temperatures and recession rates. Furthermore, none of the measured recession rates of specimens which did not ignite, except that at 1835° K, deviate from the corresponding values predicted by equation (7) by a factor greater than 3.3. On the average the agreement is somewhat better than this – a factor of about 2. This agreement is quite reasonable, as high-temperature kinetics studies go, even under more idealized circumstances; for example, Gulbransen, Andrew, and Brassart, studying the oxidation of molybdenum under laboratory conditions and considering only the special case of chemical control, also obtained differences between theory and experiment by a factor of about 3 (ref. 12). It should be noted that in the present investigation purely chemical control was not maintained; the degree of transport influence, calculated by using equations (7), (8), and (9), was 11 percent at 1535° K and 29 percent at 1965° K.

In contrast with the behavior of those specimens which oxidized normally, the experimentally determined recession rates of the few specimens which ignited are much higher than the corresponding theoretical values calculated by means of equation (7). Furthermore, the experimentally determined values are almost certainly low, as pointed out in the section "Experimental and Analytical Techniques."

The behavior of the specimens that ignited can best be understood by considering the nature of the phenomenon of ignition. According to Hill, Adamson, Foland, and Bressette (ref. 13) ignition occurs when the rate of heat input to an oxidizing surface due to its own exothermic reaction exceeds the rate of heat removal from the surface. A characteristic of ignition is a rapid increase in the temperature of the surface until some mechanism – frequently melting – comes into effect to bring the heat input and removal into balance again. The rapid rise in temperature which is characteristic of ignition was observed in this investigation; this is shown in figure 4 in which temperature is plotted against time for three of the four specimens that ignited and also for one specimen that reached a high steady-state temperature but did not ignite. (A temperature-time record was not obtained for one specimen that ignited.) The zero of time as plotted in figure 4 is not absolute for any of the specimens but has been chosen in each case so as to produce the maximum overlap among the data points at lower temperatures. Significant overlap

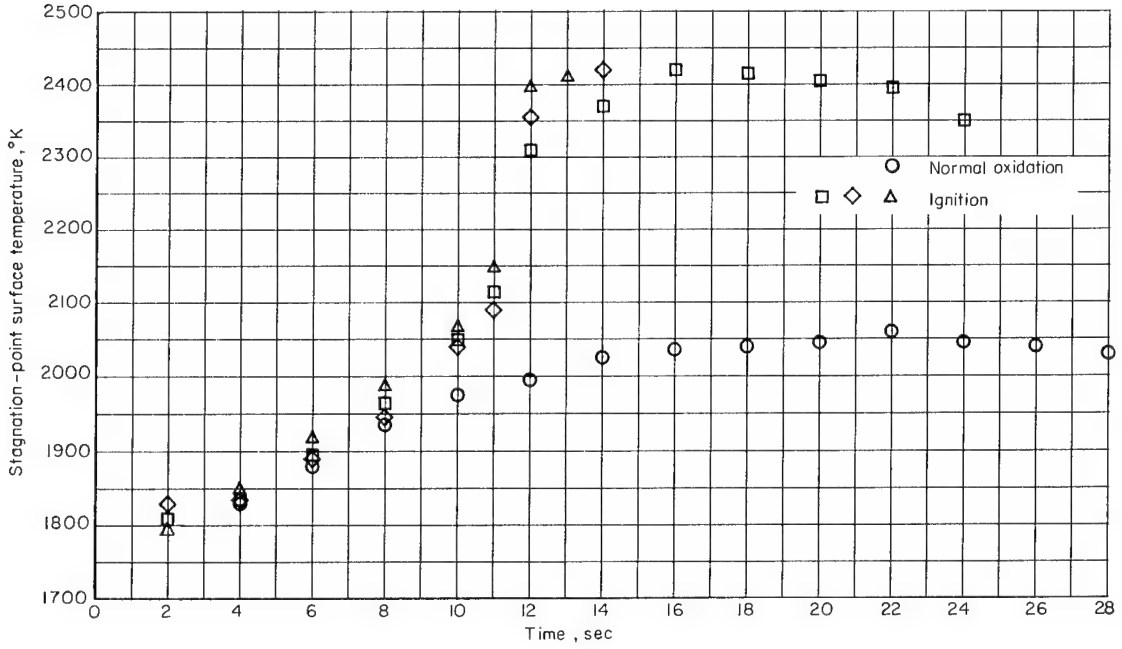

Figure 4.- Variation of stagnation-point surface temperature with time.

is evident up to about 1950° K but above this temperature the two sets of data begin to diverge. As time increases, the temperature of the normally oxidizing specimen gradually levels out; the temperature of the specimens which ignited continues to increase steadily for a short time until at about 2100° K a sharp rise of 195° K to 265° K occurs in approximately 1 second.

That melting occurred with the specimens which ignited in this investigation is illustrated in figures 5 and 6. In figure 5 molten material can clearly be seen flowing back from the nose of a specimen which had just ignited. In figure 6 the specimens which ignited can be seen to have undergone significant alteration of their original configuration, whereas the

Figure 5.- Specimen undergoing ignition. L-65-9024

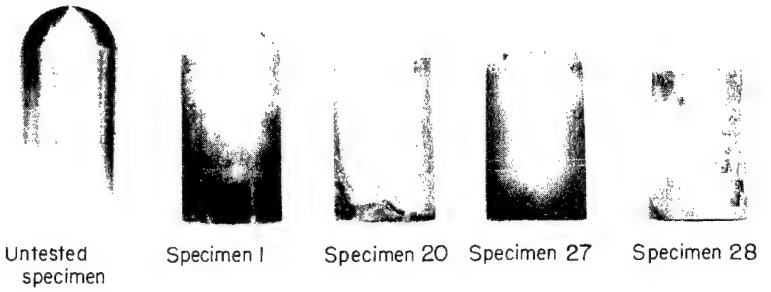

(a) Normal oxidation. L-64-11,725.1

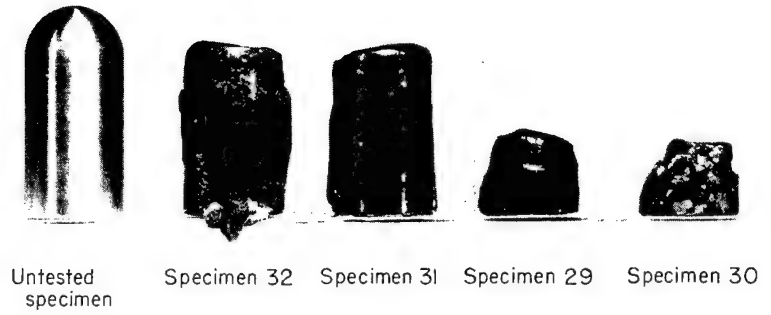

(b) Ignition. L-64-11,724.1

Figure 6.- Specimens after testing.

specimens which did not ignite retained substantially their original shape despite having undergone measurable recession. Also, two specimens which ignited have deposits of molten material on their sides which apparently flowed back from the region where melting occurred and solidified after the specimens were removed from the heated air-stream. The other two specimens were virtually destroyed and the deposit of molten material on their sides is difficult to observe.

Inasmuch as the removal of molybdenum from the nose of those specimens which ignited was caused by melting as well as by oxidation, it is not surprising that the measured recession rates of these specimens are considerably higher than the rates predicted by a mechanism that considers oxidation alone.

It is not known why the temperature at which melting occurred was determined to be about 500° K below the normal melting point of molybdenum. Errors in temperature measurement may account for some of the difference since the presence of a molten film undoubtedly changes somewhat the emissivity of the surface observed. However, a

temperature error of about 20 percent is unlikely. It is probable that the formation of a solution of metal and oxide occurs at the specimen surface, which lowers the melting point below that of pure molybdenum.

Also uncertain is the reason that some specimens which ignited did so under conditions apparently no more severe than those experienced by other specimens which did not ignite. (See table I.) It is known from unpublished tests carried out in the Langley arc-heated materials jet that at sufficiently severe conditions (Mach 2, 2535° K to 2870° K free-stream stagnation temperature, and 1.07×10^6 N-m^{-2} stagnation pressure) ignition occurs consistently. On the other hand, none of the tests reported in references 2, 3, 4, and 6, all of which involved subsonic or static conditions and gas temperatures of less than 2100° K, resulted in ignition. Apparently the conditions employed in the present investigation lie in a transition region between consistent normal oxidation and consistent ignition. In this region small differences in heat input and/or heat removal may determine whether a specimen ignites or behaves normally.

CONCLUDING REMARKS

A rate equation for the oxidation of molybdenum to its trioxide, applicable at temperatures at which the trioxide is volatile, has been derived theoretically; this equation takes into account the effects of both chemical and mass-transfer parameters. The equation is more general than a similar equation presented in NASA Technical Note D-222 and should, in fact, be applicable to any situation where the mass-transfer coefficient of oxygen to a molybdenum surface can be determined. The equation has been applied to low flow velocity data contained in the aforementioned Technical Note and values for the activation energy of the oxidation of molybdenum to its trioxide have been obtained. The standard deviation among the values is 2.1 percent and the average value of 8.51×10^7 J-(kg-mole)$^{-1}$ (20.3 kcal-(g-mole)$^{-1}$) is within 3 percent of the value 8.25×10^7 J-(kg-mole)$^{-1}$ (19.7 kcal-(g-mole)$^{-1}$) determined by Gulbransen, Andrew, and Brassart (Journal of the Electrochemical Society, September 1963) by a conventional Arrhenius plot using data obtained under predominantly chemically controlled conditions.

The theoretically derived rate equation has also been applied to the oxidation of molybdenum hemisphere-cylinders in heated Mach 2.1 airstreams at 1.07×10^6 N-m^{-2} free-stream stagnation pressure. For specimens with stagnation-point surface temperatures remaining below about 2100° K, the recession rates predicted theoretically by the derived rate equation agreed, on the average, within a factor of about 2 with the rates

determined experimentally. Specimens with stagnation-point surface temperatures rising above 2100° K ignited. This ignition was found to be characterized by a rapid rise in specimen surface temperature until melting occurred and, as might be expected, resulted in recession rates considerably in excess of those accountable by oxidation alone.

Langley Research Center,
National Aeronautics and Space Administration,
Langley Station, Hampton, Va., November 10, 1965.

APPENDIX A

CALCULATION OF MASS-TRANSFER COEFFICIENTS

Analogy Between Mass Transfer and Heat Transfer

The phenomenon of heat transfer across an enthalpy or temperature gradient has been investigated extensively and heat-transfer coefficients are available for a large variety of experimental situations. Mass-transfer coefficients, on the other hand, are less readily available. However, for certain situations mass-transfer coefficients can be obtained from known heat-transfer coefficients by means of analogies which exist between mass transfer and heat transfer for these situations. Two forms of mass-heat transfer analogy which were utilized in this investigation are derived and discussed in this appendix.

Consider a binary, compressible, laminar boundary layer in which no homogeneous chemical reactions occur. The governing equations, as developed in reference 14, are as follows:

Continuity equation

$$\frac{\partial}{\partial x}\left(\rho u r^K\right) + \frac{\partial}{\partial y}\left(\rho v r^K\right) = 0 \tag{A1}$$

where $K = 0$ for a two-dimensional body and $K = 1$ for a body of revolution.

Momentum equation

$$\rho\left(u \frac{\partial u}{\partial x} + v \frac{\partial u}{\partial y}\right) = - \frac{dp_e}{dx} + \frac{\partial}{\partial y}\left(\mu \frac{\partial u}{\partial y}\right) \tag{A2}$$

Energy equation

$$\rho\left(u \frac{\partial H_t}{\partial x} + v \frac{\partial H_t}{\partial y}\right) = \frac{\partial}{\partial y}\left(\frac{\mu}{N_{Pr}} \frac{\partial H_t}{\partial y}\right) + \frac{\partial}{\partial y}\left[\mu\left(1 - \frac{1}{N_{Pr}}\right)\frac{\partial}{\partial y}\left(\frac{u^2}{2}\right)\right] + \frac{\partial}{\partial y}\left[\rho D\left(1 - \frac{1}{N_{Le}}\right)\sum_i H_i \frac{\partial w_i}{\partial y}\right] \tag{A3}$$

Continuity equation for each species

$$\rho\left(u \frac{\partial w_i}{\partial x} + v \frac{\partial w_i}{\partial y}\right) - \frac{\partial}{\partial y}\left(\frac{\mu}{N_{Sc}} \frac{\partial w_i}{\partial y}\right) = 0 \tag{A4}$$

Consider the last two terms on the right-hand side of equation (A3). The next to last term represents heat generated by viscous shear stresses in the boundary layer, and the last term represents heat transfer by diffusion. Note that when these two terms are

negligible, equations (A3) and (A4) are of similar form. If these two equations (with the dissipation and diffusion terms of equation (A3) neglected) are expressed in terms of the dimensionless variables

$$\theta = \left(\frac{H_t - H_{t,w}}{H_{t,w} - H_{t,e}}\right) \tag{A5}$$

$$\phi_i = \left(\frac{w_i - w_{i,w}}{w_{i,e} - w_{i,w}}\right) \tag{A6}$$

the similarity of form is maintained and, in addition, the boundary conditions on the dependent variables are the same – that is,

$$\rho\left(u\frac{\partial\theta}{\partial x} + v\frac{\partial\theta}{\partial y}\right) = \frac{\partial}{\partial y}\left(\frac{\mu}{N_{Pr}}\frac{\partial\theta}{\partial y}\right) \tag{A7}$$

$$\rho\left(u\frac{\partial\phi_i}{\partial x} + v\frac{\partial\phi_i}{\partial y}\right) = \frac{\partial}{\partial y}\left(\frac{\mu}{N_{Sc}}\frac{\partial\phi_i}{\partial y}\right) \tag{A8}$$

and

$$\theta = \phi_i = 0 \qquad (y = 0) \tag{A9}$$

$$\theta = \phi_i \to 1 \qquad (y \to \infty) \tag{A10}$$

If the Lewis number is unity $(N_{Pr} = N_{Sc})$, equations (A7) and (A8) are not just similar in form but are identical and, hence, $\theta = \phi_i$.

Therefore,

$$\left(\frac{\partial\theta}{\partial y}\right)_w = \left(\frac{\partial\phi_i}{\partial y}\right)_w \tag{A11}$$

From Fourier's law of conduction and the definition of the heat-transfer coefficient

$$q_w = -\left(\frac{\kappa}{\bar{c}_p}\right)_w \left(H_{t,e} - H_{t,w}\right)\left(\frac{\partial\theta}{\partial y}\right)_w = h\left(H_{t,e} - H_{t,w}\right) \tag{A12}$$

and from Fick's first law of diffusion and the definition of the mass-transfer coefficient

$$\dot{m}_{i,w} = -\rho_w D_w\left(w_{i,e} - w_{i,w}\right)\left(\frac{\partial\phi_i}{\partial y}\right)_w = h_D\left(w_{i,e} - w_{i,w}\right) \tag{A13}$$

Hence,

$$\frac{h_D}{\rho_w D_w} = \frac{h\bar{c}_{p,w}}{\kappa_w} \tag{A14}$$

Equation (A14) is a statement of the mass-heat transfer analogy for situations in which simultaneous mass and heat transfer are involved. It must be remembered that this analogy is rigorously valid only when $N_{Le} = 1$ (note that this condition, in addition to specifying the equality of the Schmidt and Prandtl numbers, eliminates the diffusion term in equation (A3)) and there is no appreciable heat generation in the boundary layer due to viscous sheer stresses. The latter condition is met whenever the local flow velocity is small compared with the velocity of sound. This is the case for all points on a body situated in a low subsonic flow stream but for transonic and supersonic flow streams it is the case only near the stagnation point. The requirement that $N_{Le} = 1$ is seldom met exactly but is generally assumed to be satisfied for values between about 0.7 and 1.5. Air over a large range of temperatures and pressures meets this less stringent requirement as do a number of other gas mixtures (ref. 14).

A somewhat modified form of mass-heat transfer analogy can be derived for the special case of mass transfer through a boundary layer within which no heat transfer takes place without assuming the Lewis number to be unity. The governing equations for this special case are equations (A1), (A2), and (A8). Because there is no heat transfer in the boundary layer, equation (A7) is eliminated.

In the development of this form of analogy it is necessary to consider another special case – namely, the transfer of heat through a boundary layer within which no mass transfer or viscous dissipation takes place. For this case equations (A1), (A2), and (A7) are the governing equations and equation (A8) is eliminated. The two special cases can be seen to be similar since they have equations (A1) and (A2) in common and equations (A7) and (A8) differ only in their dimensionless terms $(\theta, \ \phi, \ N_{Pr}$, and $N_{Sc})$. If both the Schmidt number and the Prandtl number are independent of x and y, then any solution to equation (A7) can be transformed into a solution to equation (A8) by replacing the Prandtl number, wherever it appears, by the Schmidt number. Obviously, a similar transformation exists between $\left(\frac{\partial\theta}{\partial y}\right)_w$ and $\left(\frac{\partial\phi_i}{\partial y}\right)_w$ and, hence, in view of equations (A12) and (A13), between $\frac{h_D}{\rho_w D_w}$ and $\frac{h\bar{c}_{p,w}}{\kappa_w}$. This transformation form of mass-heat transfer analogy is equivalent to that presented by Eckert in reference 15.

As stated previously this form of analogy cannot be applied to situations in which both mass transfer and heat transfer occur simultaneously to a significant extent. In addition, since the Prandtl and Schmidt numbers have been assumed to be independent of x and y, the composition of the gas must be relatively homogeneous throughout the

boundary layer. This assumption is, of course, met when the rate of reaction of oxygen at the surface is slow compared with the replenishment rate or, in other words, when the reaction is essentially chemically controlled. When chemical control does not apply, homogeneity can still be approximated by the presence of a large percentage of inert gas. Finally, as was the case with the first form of analogy derived, the local Mach number must be relatively small.

Thin Flat Plates

The thin flat-plate specimens, the oxidation rates of which are presented in reference 2 and reproduced herein in table II, were oxidized under conditions such that heat transfer within the boundary layer was negligible. The specimens were oxidized in flowing gas streams with very low flow velocities, of the order of 1 to 10 m-sec^{-1}. The gas mixtures used were air and two helium-oxygen mixtures, all of which had at least 79 mole percent inert constituents. In view of these conditions, mass-transfer coefficients for these specimens can be obtained from related heat-transfer coefficients by means of the second form of mass-heat transfer analogy derived.

Heat-transfer coefficients (as defined in this report) are related to Nusselt numbers by the following equation:

$$N_{Nu} = \frac{h\bar{c}_{p,w}x}{\kappa_w} \tag{A15}$$

The Nusselt number for a thin flat plate in laminar flow is given in reference 15 as

$$N_{Nu} = 0.332 \sqrt[3]{N_{Pr}} \sqrt{N_{Re}} \tag{A16}$$

Combining equations (A15) and (A16) and dividing by x yields

$$\frac{h\bar{c}_{p,w}}{\kappa_w} = \frac{0.332}{x} \sqrt[3]{N_{Pr}} \sqrt{N_{Re}} \tag{A17}$$

According to the applicable analogy equation (A17) may be transformed as follows:

$$\frac{h_D}{\rho_w D_w} = \frac{0.332}{x} \sqrt[3]{N_{Sc}} \sqrt{N_{Re}} \tag{A18}$$

Therefore,

$$h_D = 0.332 \frac{\rho_w D_w}{x} \sqrt[3]{N_{Sc}} \sqrt{N_{Re}} \tag{A19}$$

APPENDIX A

Hemisphere-Cylinders

The hemisphere-cylinders tested in this investigation were oxidized under conditions such that the amount of heat transfer which accompanied the mass transfer was not negligible. The only gas mixture used was air for which the Lewis number at the temperatures and pressures involved is reasonably close to unity (ref. 14). Oxidation rates were determined only at the stagnation point of the specimens. These considerations point to the use of the first form of mass-heat transfer analogy derived, as expressed by equation (A14).

From the definition of the Nusselt and Reynolds numbers

$$\frac{h\bar{c}_{p,w}}{\kappa_w} = \frac{N_{Nu,w}}{\sqrt{N_{Re,w}}}\left(\frac{N_{Ma,w}a_w\rho_w}{\mu_w x}\right)^{1/2} \tag{A20}$$

Combining equations (A14) and (A20) gives

$$\frac{h_D}{\rho_w D_w} = \frac{N_{Nu,w}}{\sqrt{N_{Re,w}}}\left(\frac{N_{Ma,w}a_w\rho_w}{\mu_w x}\right)^{1/2} \tag{A21}$$

In reference 16 is presented a plot of $N_{Ma,w}$ against x/d for each of several free-stream Mach numbers greater than 1. In the stagnation region all the curves asymptotically approach a straight line passing through the origin with a slope of 2.4. Therefore, in the stagnation region for free-stream Mach numbers greater than 1 the local Mach number is independent of the free-stream Mach number and is given by the expression

$$N_{Ma,w} = \frac{2.4x}{d} \tag{A22}$$

Substitution of equation (A22) into equation (A21) yields

$$\frac{h_D}{\rho_w D_w} = \frac{N_{Nu,w}}{\sqrt{N_{Re,w}}}\left(\frac{2.4a_w\rho_w}{\mu_w d}\right)^{1/2} \tag{A23}$$

Therefore,

$$h_D = \frac{N_{Nu,w}D_w}{\sqrt{N_{Re,w}}}\left(\frac{2.4a_w\rho_w^3}{\mu_w d}\right)^{1/2} \tag{A24}$$

APPENDIX A

Reference 17 presents a series of plots of $N_{Nu,w}/\sqrt{N_{Re,w}}$ at the stagnation point of an axially symmetric body as a function of T_w/T_e for each of several values of the Prandtl number. These plots are represented quite well by the equation

$$\frac{N_{Nu,w}}{\sqrt{N_{Re,w}}} = \left[0.7 + 0.064\left(\frac{T_w}{T_e}\right)^{0.9}\right] N_{Pr}^{0.4} \tag{A25}$$

Therefore,

$$h_D = \left[0.7 + 0.064\left(\frac{T_w}{T_e}\right)^{0.9}\right] N_{Pr}^{0.4}\, D_w \left(\frac{2.4 a_w \rho_w^3}{\mu_w d}\right)^{1/2} \tag{A26}$$

Since this expression for the mass-transfer coefficient is relatively insensitive to T_w/T_e, this ratio was assumed to be unity in the determination of the theoretical curve presented in figure 3 of this report.

APPENDIX B

VALUES OF PARAMETERS EMPLOYED IN COMPUTATIONS

In the application of various equations presented in this report it is necessary to have values for the parameters E_a, ρ, $\overline{U}$, D, μ, a, $\bar{c}_p$, and κ. The values and equations for these parameters which were employed in this investigation are given in this appendix.

Activation Energy

The activation energy was assumed to be 8.55×10^7 J-(kg-mole)$^{-1}$ (20.3 kcal-(g-mole)$^{-1}$). This is the average value determined by means of equation (16) from the data presented in reference 2.

Density

The equation for the density was obtained by a rearrangement of the ideal gas equation – that is

$$\rho = \frac{mp}{RT} \tag{B1}$$

The molecular weights of the mixtures were taken to be the averages of the molecular weights of the individual gases, weighted according to their mole fractions.

Average Velocity of Oxygen Molecules

The equation used for the average velocity of oxygen molecules is that derived in the kinetic theory of gases. (See, for example, ref. 8.) It is

$$\overline{U} = \left(\frac{8RT}{\pi m_{O_2}}\right)^{1/2} \tag{B2}$$

Diffusivity

A semiempirical equation for the diffusivity of various binary gas mixtures is given in reference 18 – namely,

$$D = D_O\left(\frac{T}{T_O}\right)^n \frac{p_O}{p} \tag{B3}$$

The standard temperature T_O and standard pressure p_O employed in reference 18 are 273° K and 1.013×10^5 N-m^{-2} (1 atm), respectively. The constants D_O and n are

given for a number of gas mixtures, including air. Substitution of the values given for T_o, p_o, D_o, and n into equation (B3) and multiplication by a conversion factor to yield units of meters^2 per second produces the equation

$$D_{air} = \frac{1.00 \times 10^{-4} T^{1.75}}{p} \tag{B4}$$

Reference 18 does not give the values of D_o and n for oxygen-helium mixtures. However, n was assumed to be 1.75 since this is the value given for nearly two-thirds of the mixtures cited, including the only mixture containing helium (helium-argon). A value for D_o was obtained for the oxygen-helium mixtures by means of a relationship presented in reference 19. In this reference the diffusivity of binary gas mixtures is represented by an expression similar to equation (B3). The term corresponding to D_o is proportional to the parameter $\left(\frac{1}{m_1} + \frac{1}{m_2}\right)^{1/2} \Big/ \left(V_1^{1/3} + V_2^{1/3}\right)^2$. Evaluation of the ratio of the value of this parameter for one gas mixture to its value for a second gas mixture should yield the ratio of the values of D_o for the two mixtures and, hence, if the value of D_o is known for one of the mixtures, its value for the other can be determined. Employing this scheme and using the known value of D_o for air gives the following equation:

$$D_{O_2,He} = 2.22 \times 10^{-4} \frac{T^{1.75}}{p} \tag{B5}$$

Viscosity

Reference 18 gives the following semiempirical equation for the viscosity of certain gases:

$$\mu = \frac{a_o T^{1/2}}{1 + \frac{a_2 10^{-a_1/T}}{T}} \tag{B6}$$

If the values for the constants a_o, a_1, and a_2 which are given in this reference for air are substituted into equation (B6) and an appropriate factor is introduced to convert the viscosity from poise to newtons per meter^2 per second, the following equation is obtained:

$$\mu_{air} = \frac{1.488 \times 10^{-6} T^{1/2}}{1 + \frac{122.1 \times 10^{-5/T}}{T}} \tag{B7}$$

Values of the constants in equation (B6) are not given in reference 18 for oxygen-helium mixtures and, hence, this equation could not be applied to these mixtures.

However, reference 19 gives a general equation for the viscosity of a binary gas mixture which is applicable, in principle, to any pair of gases with known individual viscosities. This equation is

$$\mu_{12} = \frac{\mu_1}{1 + \frac{1}{2\sqrt{2}} \frac{X_2}{X_1} \frac{\left[1 + (\mu_1/\mu_2)^{1/2}(m_2/m_1)^{1/4}\right]^2}{(1 + m_1/m_2)^{1/2}}} + \frac{\mu_2}{1 + \frac{1}{2\sqrt{2}} \frac{X_1}{X_2} \frac{\left[1 + (\mu_2/\mu_1)^{1/2}(m_1/m_2)^{1/4}\right]^2}{(1 + m_2/m_1)^{1/2}}} \tag{B8}$$

The individual viscosities of oxygen and helium were not obtained from equation (B6) although the values of a_0, a_1, and a_2 for these gases are presented in reference 18, because the temperature range of applicability cited for these two gases is too restricted.

The equation used for the viscosity of helium was obtained from reference 20. With appropriate conversion of units it is

$$\mu_{He} = \frac{4.230 \times 10^{-7} T^{3/2}}{T^{0.826} - 0.409} \tag{B9}$$

Sutherland's equation (see ref. 19) was used for the viscosity of oxygen. The constants in Sutherland's equation were obtained by fitting the equation to the viscosity values presented in reference 21. The resulting equation is

$$\mu_{O_2} = \frac{1.612 \times 10^{-6} T^{1/2}}{1 + \frac{17.95}{T}} \tag{B10}$$

Speed of Sound

The equation used for the speed of sound in air is

$$a_{air} = 25.30 T_w^{0.4636} \tag{B11}$$

This equation is an empirical fit to tabulated values presented in reference 21.

APPENDIX B

Specific Heat

The equation used for the specific heat of air at constant pressure is

$$\bar{c}_{p,air} = 9.781 \times 10^{2} + 0.1718T_{w} \tag{B12}$$

Equation (B12) is also an empirical fit to tabulated values presented in reference 21.

Thermal Conductivity

The equation used for the thermal conductivity of air is

$$\kappa_{air} = 8.476 \times 10^{-3} + 6.266 \times 10^{-5}T_{w} - 8.501 \times 10^{-9}T_{w}^{2} \tag{B13}$$

This equation is an empirical fit to tabulated values presented in reference 22.

REFERENCES

1. Promisel, N. E., ed.: The Science and Technology of Tungsten, Tantalum, Molybdenum, Niobium and Their Alloys. AGARDograph 82, Pergamon Press, c.1964.

2. Modisette, Jerry L.; and Schryer, David R.: An Investigation of the Role of Gaseous Diffusion in the Oxidation of a Metal Forming a Volatile Oxide. NASA TN D-222, 1960.

3. Gulbransen, E. A.; Andrew, K. F.; and Brassart, F. A.: Oxidation of Molybdenum 550° to 1700° C. J. Electrochem. Soc., vol. 110, no. 9, Sept. 1963, pp. 952-959. (Discussion by D. R. Schryer, J. Electrochem. Soc., vol. 111, no. 6, June 1964, pp. 757-759.)

4. Wilks, C. R.: Effect of Temperature, Pressure, and Mass-Flow on the Oxidation Rate of Molybdenum. ER 10643-2, The Martin Co., Dec. 31, 1959.

5. Rosner, Daniel E.: The Apparent Chemical Kinetics of Surface Reactions in External Flow Systems – Diffusional Falsification of Activation Energy and Reaction Order. TP-35, AeroChem Res. Labs., Inc., Aug. 1, 1961.

6. Bartlett, E. S.; and Williams, D. N.: The Oxidation Rate of Molybdenum in Air. Trans. Met. Soc. AIME, vol. 212, no. 2, Apr. 1958, pp. 280-281.

7. Laidler, K. J.; Glasstone, S.; and Eyring, H.: Application of the Theory of Absolute Reaction Rates to Heterogeneous Processes. I. The Adsorption and Desorption of Gases. J. Chem. Phys., vol. 8, no. 9, Sept. 1940, pp. 659-667.

8. Kennard, Earle H.: Kinetic Theory of Gases. McGraw-Hill Book Co., Inc., 1938.

9. Trout, Otto F., Jr.: Design, Operation, and Testing Capabilities of the Langley 11-Inch Ceramic-Heated Tunnel. NASA TN D-1598, 1963.

10. Exton, Reginald J.: Theory and Operation of a Variable Exposure Photographic Pyrometer Over the Temperature Range 1800° to 3600° F (1255° to 2255° K). NASA TN D-2660, 1965.

11. Siviter, James H., Jr.; and Strass, H. Kurt: An Investigation of a Photographic Technique of Measuring High Surface Temperatures. NASA TN D-617, 1960.

12. Gulbransen, E. A.; Andrew, K. F.; and Brassart, F. A.: Oxidation of Graphite, Molybdenum and Tungsten at 1000 to 1600° C. Preprint No. 63-493, Am. Inst. Aeron. Astronaut., Dec. 1963.

13. Hill, Paul R.; Adamson, David; Foland, Douglas H.; and Bressette, Walter E.: High-Temperature Oxidation and Ignition of Metals. NACA RM L55L23b, 1956.

14. Lees, Lester: Convective Heat Transfer With Mass Addition and Chemical Reactions. Combustion and Propulsion – Third AGARD Colloquium, M. W. Thring, O. Lutz, J. Fabri, and A. H. Lefebvre, eds., Pergamon Press, 1958, pp. 451-498.

15. Eckert, E. R. G. (With Pt. A and Appendix by Robert M., Drake, Jr.): Heat and Mass Transfer. Second ed. of Introduction to the Transfer of Heat and Mass, McGraw-Hill Book Co., Inc., 1959.

16. Stine, Howard A.; and Wanlass, Kent: Theoretical and Experimental Investigation of Aerodynamic-Heating and Isothermal Heat-Transfer Parameters on a Hemispherical Nose With Laminar Boundary Layer at Supersonic Mach Numbers. NACA TN 3344, 1954.

17. Reshotko, Eli; and Cohen, Clarence B.: Heat Transfer at the Forward Stagnation Point of Blunt Bodies. NACA TN 3513, 1955.

18. Gray, Dwight E., coordinating ed.: American Institute of Physics Handbook. McGraw-Hill Book Co., Inc., 1957.

19. Reid, Robert C.; and Sherwood, Thomas K.: The Properties of Gases and Liquids. McGraw-Hill Book Co., Inc., 1958.

20. Nuttall, R. L.: The NBS-NACA Tables of Thermal Properties of Gases. Table 6.39 Helium – Coefficient of Viscosity. Natl. Bur. Std., U.S. Dept. Com., Dec. 1950.

21. Hilsenrath, Joseph; Beckett, Charles W.; et al.: Tables of Thermal Properties of Gases. NBS Circ. 564, U.S. Dept. Com., 1955.

22. Hansen, C. Frederick: Approximations for the Thermodynamic and Transport Properties of High-Temperature Air. NASA TR R-50, 1959. (Supersedes NACA TN 4150.)

TABLE I.- TEST CONDITIONS, DATA, AND CALCULATIONS FOR MOLYBDENUM HEMISPHERE-CYLINDERS TESTED IN LANGLEY 11-INCH CERAMIC-HEATED TUNNEL

[Free-stream stagnation pressure, 1.07×10^6 N-m^{-2}; Mach number, 2.1]

(a) 40-second tests

Specimen (a)	Free-stream stagnation temperature, T_t, °K	Total recession, m	Average of stagnation-point surface temperature at 30 and 40 sec, $\overline{T}_{30\text{-}40}$, °K
1	1765	0.41×10^{-3}	1635
2	1765	.46	1680
3	1805	.51	1760
4	1805	.53	1705
5	1810	1.07	1860
6	1855	1.27	1960
7	1865	1.45	2035

[a]Specimens are numbered for convenience in identification and these numbers do not indicate the order in which specimens were tested.

TABLE I.- TEST CONDITIONS, DATA, AND CALCULATIONS FOR MOLYBDENUM HEMISPHERE-CYLINDERS TESTED IN LANGLEY 11-INCH CERAMIC-HEATED TUNNEL – Continued

[Free-stream stagnation pressure; 1.07×10^6 N-m^{-2}; Mach number, 2.1]

(b) Nonignition tests longer than 40 seconds

Specimen (a)	Free-stream stagnation temperature, T_t, ^oK	Test time, sec	Total recession, m	Average of stagnation-point surface temperature at 30 and 40 sec, $\overline{T}_{30-40}$, ^oK	Average steady-state stagnation-point surface temperature from 40 sec to end of test, $\overline{T}$, ^oK	Recession rate, m-sec^{-1}
8	1780	90	0.56×10^{-3}	1600	1535	0.71×10^{-5}
9	1780	150	1.24	1610	1560	.91
10	1920	180	2.51	1785	1765	1.27
11	1920	220	2.51	1550	1580	1.35
12	1805	150	1.80	1530	1545	1.65
13	2020	150	2.11	1640	1640	1.63
14	2020	90	1.27	1745	1740	1.27
15	2030	150	2.01	1620	1635	1.57
16	2035	90	1.19	1705	1695	1.37
17	2045	90	1.32	1855	1835	.71
18	2055	120	3.07	1765	1795	2.95
19	2060	120	3.20	1665	1770	3.51
20	2060	80	1.91	1865	1840	2.29
21	2065	80	2.08	1855	1805	2.79
22	2065	120	3.30	1895	1860	2.79
23	2105	80	3.61	2010	1955	5.46
24	2105	80	1.73	1870	1825	1.78
25	2110	80	1.55	1735	1765	2.36
26	2110	120	3.94	1965	1905	3.30
27	2115	120	2.64	1815	1785	2.26
28	2120	120	4.72	2080	1965	3.89

[a]Specimens are numbered for convenience in identification and these numbers do not indicate the order in which specimens were tested.

TABLE I.- TEST CONDITIONS, DATA, AND CALCULATIONS FOR MOLYBDENUM HEMISPHERE-CYLINDERS TESTED IN LANGLEY 11-INCH CERAMIC-HEATED TUNNEL – Concluded

[Free-stream stagnation pressure, 1.07×10^6 N-m^{-2}; Mach number, 2.1]

(c) Ignition tests

Specimen (a)	Free-stream stagnation temperature, T_t, ^oK	Total test time, sec	Duration of ignition, sec	Total recession, m	Average preignition stagnation-point surface temperature, ^oK	Average temperature following ignition, ^oK	Ignition recession rate, m-sec^{-1}
29	1870	<180	21	11.13×10^{-3}	1630	2365	35.3×10^{-5}
30	2020	<40	(b)	11.10	(b)	(b)	(b)
31	2055	28	4	3.05	1765	2395	51.6
32	2060	26	3	2.92	1825	2405	62.5

[a]Specimens are numbered for convenience in identification and these numbers do not indicate the order in which specimens were tested.

[b]Not available.

TABLE II.- EXPERIMENTAL DATA AND CALCULATED ACTIVATION ENERGY VALUES FOR OXIDATION OF THIN FLAT PLATES OF MOLYBDENUM IN TUBE FURNACE

Wall temperature, T_w, ^oK (a)	Flow velocity, u_e, $m\text{-}sec^{-1}$ (a)	Average oxidation rate, k_{av}, $kg\text{-}m^{-2}\text{-}sec^{-1}$ (a)	Specimen dimensions, cm (a)	Activation energy, E_a, $J\text{-}(kg\text{-}mole)^{-1}$ (b)
Series 1; air; volumetric flow rate, 0.57×10^{-4} $m^3\text{-}sec^{-1}$				
1322	1.76	2.96×10^{-3}	$2.49 \times 1.14 \times 0.25$	8.326×10^7
1369	1.83	3.10	$2.49 \times 1.14 \times 0.25$	8.496
1425	1.90	3.32	$2.49 \times 1.14 \times 0.25$	8.643
1486	1.98	4.05	$2.49 \times 1.14 \times 0.25$	8.296
1514	2.01	4.23	$2.49 \times 1.14 \times 0.25$	8.275
Series 2; air; volumetric flow rate, 1.09×10^{-4} $m^3\text{-}sec^{-1}$				
1314	3.35	3.25×10^{-3}	$2.46 \times 1.14 \times 0.25$	8.459×10^7
1347	3.44	3.18	$2.46 \times 1.14 \times 0.25$	8.717
1386	3.54	3.76	$2.46 \times 1.14 \times 0.25$	8.589
1436	3.67	4.40	$2.46 \times 1.14 \times 0.25$	8.489
1450	3.71	4.86	$2.46 \times 1.14 \times 0.25$	8.268
1478	3.78	4.91	$2.46 \times 1.14 \times 0.25$	8.396

[a]From reference 2.

[b]Calculated by equation (16).

TABLE II.- EXPERIMENTAL DATA AND CALCULATED ACTIVATION ENERGY VALUES FOR OXIDATION OF THIN FLAT PLATES OF MOLYBDENUM IN TUBE FURNACE – Concluded

Wall temperature, T_w, ^oK (a)	Flow velocity, u_e, $m\text{-}sec^{-1}$ (a)	Average oxidation rate, k_{av}, $kg\text{-}m^{-2}\text{-}sec^{-1}$ (a)	Specimen dimensions, cm (a)	Activation energy, E_a, $J\text{-}(kg\text{-}mole)^{-1}$ (b)
Series 3; air; volumetric flow rate, 1.49×10^{-4} $m^3\text{-}sec^{-1}$				
1300	4.55	3.20×10^{-3}	$2.46 \times 1.14 \times 0.25$	8.526×10^7
1350	4.72	3.57	$2.46 \times 1.14 \times 0.25$	8.640
1369	4.79	3.52	$2.46 \times 1.14 \times 0.25$	8.787
1400	4.90	4.15	$2.46 \times 1.17 \times 0.25$	8.626
1425	4.99	4.74	$2.46 \times 1.14 \times 0.25$	8.457
1455	5.10	5.08	$2.46 \times 1.14 \times 0.25$	8.450
Series 4; 21.5% 0_2, 78.5% He; volumetric flow rate, 1.34×10^{-4} $m^3\text{-}sec^{-1}$				
1306	4.12	4.42×10^{-3}	$2.36 \times 1.19 \times 0.25$	8.373×10^7
1329	4.19	4.71	$2.46 \times 1.35 \times 0.25$	8.401
1362	4.29	5.18	$2.39 \times 1.14 \times 0.25$	8.440
1396	4.40	5.84	$2.39 \times 1.14 \times 0.25$	8.415
1478	4.66	7.13	$2.41 \times 1.14 \times 0.25$	8.452
Series 5; 13.6% 0_2, 86.4% He; volumetric flow rate, 2.07×10^{-4} $m^3\text{-}sec^{-1}$				
1433	6.97	3.47×10^{-3}	$2.41 \times 1.14 \times 0.25$	8.873×10^7
1462	7.11	3.81	$2.39 \times 1.14 \times 0.25$	8.877
1539	7.49	5.35	$2.39 \times 1.14 \times 0.25$	8.594
1562	7.60	5.18	$2.46 \times 1.17 \times 0.25$	8.780
1610	7.83	6.59	$2.46 \times 1.17 \times 0.25$	8.385
1623	7.90	7.06	$2.41 \times 1.14 \times 0.25$	8.259
1644	8.00	7.38	$2.41 \times 1.14 \times 0.25$	8.215

[a]From reference 2.

[b]Calculated by equation (16).

TABLE III.- COMPARISON OF CALCULATED VALUES OF E_a

Series	Gas composition	E_a from ref. 2, J-(kg-mole)$^{-1}$	E_a from eq. (16), J-(kg-mole)$^{-1}$
1	Air	8.53×10^7	8.42×10^7
2	Air	9.00	8.49
3	Air	9.16	8.58
4	21.5% O_2, 78.5% He	8.51	8.42
5	13.6% O_2, 86.4% He	9.37	8.58
Mean value of E_a, J-(kg-mole)$^{-1}$ . .		8.91×10^7	8.51×10^7
Percent standard deviation		5.7	2.1

"The aeronautical and space activities of the United States shall be conducted so as to contribute . . . to the expansion of human knowledge of phenomena in the atmosphere and space. The Administration shall provide for the widest practicable and appropriate dissemination of information concerning its activities and the results thereof."

—NATIONAL AERONAUTICS AND SPACE ACT OF 1958

NASA SCIENTIFIC AND TECHNICAL PUBLICATIONS

TECHNICAL REPORTS: Scientific and technical information considered important, complete, and a lasting contribution to existing knowledge.

TECHNICAL NOTES: Information less broad in scope but nevertheless of importance as a contribution to existing knowledge.

TECHNICAL MEMORANDUMS: Information receiving limited distribution because of preliminary data, security classification, or other reasons.

CONTRACTOR REPORTS: Technical information generated in connection with a NASA contract or grant and released under NASA auspices.

TECHNICAL TRANSLATIONS: Information published in a foreign language considered to merit NASA distribution in English.

TECHNICAL REPRINTS: Information derived from NASA activities and initially published in the form of journal articles.

SPECIAL PUBLICATIONS: Information derived from or of value to NASA activities but not necessarily reporting the results of individual NASA-programmed scientific efforts. Publications include conference proceedings, monographs, data compilations, handbooks, sourcebooks, and special bibliographies.

Details on the availability of these publications may be obtained from:

SCIENTIFIC AND TECHNICAL INFORMATION DIVISION

NATIONAL AERONAUTICS AND SPACE ADMINISTRATION

Washington, D.C. 20546